Landslides (2009) 6:111–116
DOI 10.1007/s10346-009-0146-7
Received: 24 October 2008
Accepted: 30 January 2009
Published online: 3 March 2009


Heike Willenberg · Erik Eberhardt · Simon Loew · Scott McDougall · Oldrich Hungr

# Hazard assessment and runout analysis for an unstable rock slope above an industrial site in the Riviera valley, Switzerland

**Abstract** This paper presents a detailed field investigation and hazard assessment for an unstable rock slope above an industrial site in the Riviera valley in the Canton of Ticino in southern Switzerland. An integrated framework was used to counter issues of geological complexity and uncertainty, linking geological mapping and numerical modeling to develop an understanding of the acting instability mechanism to 2-D and 3-D dynamic runout simulations to predict the travel path and reach in the event of a large volume rockslide. The results from the numerical stability analysis provided a means to constrain failure volume estimates, whereas a series of calibration simulations were used to constrain the input parameters required by the rheological model used for the runout analysis. Results from this assessment suggest that current protection measures in place may not be sufficient, helping local authorities to define hazard zones and aid further development plans for the region.

**Keywords** Rock slope hazard · Massive crystalline rock · Numerical modeling · Runout simulation · Hazard assessment

## Introduction

Unstable rock slopes present a major hazard when they are situated above populated alpine valley areas (Petley et al. 2005; Nadim et al. 2006). In strong rock masses where steeper slopes form, failures have the potential to develop into long-runout rockslides, rock avalanches, mixed rockslide–debris avalanches, etc. (e.g., Geertsema et al. 2006), with a large destructive potential (Eisbacher and Clague 1984). Alternatively, failure may occur through a succession of smaller rockslides, collapses, and/or rockfalls. These, in general, have shorter runouts and less destructive potential, but still may cause heavy damage if infrastructure is located close to the toe of the slope or through damming of a river and subsequent flooding (e.g., Schindler et al. 1993).

This range in behavior means that to effectively mitigate the threat posed by an unstable rock slope, either through remedial measures and/or an early warning system, it becomes essential to establish the processes acting on the unstable rock volume such that the post-failure runout (i.e., travel distance and velocities) can be effectively quantified with respect to the area and infrastructure at risk (Hungr et al. 2005). However, the identification of a valid instability model depends on the amount and quality of geological information and monitoring data available for the rock slope, and this is often limited. Furthermore, the prediction of the potential failed volume required for a runout analysis becomes a further source of uncertainty because the depth of failure is typically unknown or poorly constrained.

This paper presents the results of a hazard assessment and runout analysis performed for an unstable rock slope above an industrial site near Preonzo, Switzerland. Already, two large rockslide events are known to have occurred, in 1760 and 2002, originating from the same slope. Integral to the study was the use of geological mapping and numerical modeling to gain understanding of the acting instability mechanism and to constrain potential failed volumes to be used in subsequent 2-D and 3-D runout analyses. The approach taken and results obtained are reported here. Together, these helped provide a basis for the local authorities to define hazard zones, design necessary countermeasures (e.g., early warning systems, evacuation plans, etc.), and to aid further development plans for the region.

## Site overview

The unstable rock mass is situated along the western slope of the N-S trending Riviera valley close to the village of Preonzo in southern Switzerland (Fig. 1), at an approximate elevation of 1,300 m above the valley floor. Below the potentially unstable rock slope (known locally as Alpe di Roscioro), the industrial area Sgrussa is situated (Figs. 2 and 3a). A protection berm was constructed in 2002 between a small river channel (Valegion) and the industrial area, mainly for protection against rock fall and debris flows.

## Slope instability history

The site has a long history of rock slope failures. In 1760, a large rockslide from the area of the Alpe di Roscioro is believed to have destroyed parts of Preonzo. Boulders, inferred to have originated from this rockslide (due to spatial and temporal causality), have been encountered in reconnaissance boreholes drilled for the highway, located in the middle of the valley 400 m from the foot of the slope. Since 1991, ongoing slope activity has been monitored across a large open tension crack at the top of Alpe di Roscioro (Fig. 3b). In May 2002, 150,000 $m^3$ of rock failed from the southern part of the cliff below the Alpe di Roscioro after a heavy rainfall (Fig. 2). This event occurred as a series of smaller rockfalls over a 7-h period. Most of the released rock traveled from the source area down the slope about 600 m. Some blocks reached the protection berm at Sgrussa that was then under construction. Fracture opening of the tension crack on the Alpe di Roscioro continued after the 2002 event. The front of this developing instability, which is located north of the 2002 release area, corresponds with a near-vertical cliff running parallel to the Riviera valley (Fig. 2b). However, the depth and lateral extent of the instability are not well defined.

## Geology

The Alpe di Roscioro lies within the Penninic Simano nappe composed of WSW dipping gneisses, amphibolites, and schists (Fig. 4). Lithologic contacts and foliation dip approximately 25° into the slope, kinematically favoring rock slope stability. The


**Fig. 1** Location of the study site and other rockslide case studies in Switzerland

amphibolitic gneisses and augengneisses, which form the cliff below the Alpe di Roscioro, are rather massive in the northern part and much more competent than the strongly disintegrated southern rock mass that failed in 2002. In contrast, the layered gneisses and most notably a several meter thick schist band at the base of the steep wall (Fig. 4) were assessed as being significantly weaker. Several springs have been mapped at the top of the schist band following heavy rainfall events indicating that the schist band also acts as a low permeability boundary to groundwater flow within the slope.

The local discontinuity network is dominated by three steeply dipping fracture sets and one fracture set parallel to foliation as shown in Fig. 5. Two fracture sets (K1 and K2) strike parallel to the steep slope face below the Alpe di Roscioro. The third set (K3) is oriented perpendicular to the latter. No fractures or faults were observed dipping toward the valley, which could serve as a clear basal sliding surface.

## Monitoring

The monitoring system at the Alpe di Roscioro initially consisted of a set of survey benchmark pairs across the large open tension crack behind the steep rock face (Fig. 3b). These were measured manually since 1991. The monitoring system was expanded in 1999 with automatically logged surface extensometers and geodetic surveys from the locally named Alp Cher (Fig. 2). On the basis of the early warning monitoring, the 2002 rockslide events were successfully predicted and the facilities below the rockslide area evacuated.

At present, manual tension crack measurements and automatic crack extensometers show opening rates of between 2 and 3 cm/year (Fig. 6), with periodic accelerations coinciding with heavy precipitation events. After phases of acceleration, the long-term displacement rates are nearly constant. The magnitudes of opening at the tension crack and surface displacements at the geodetically surveyed points are in general agreement. Based on these observations, it was assumed that the upper part of the unstable volume was bounded in the back by the tension crack and that the mass was moving coherently.

## Slope stability modeling

Slope stability modeling adopting a continuum approach (e.g., Stead et al. 2006) and rock mass strain weakening techniques (e.g., Eberhardt et al. 2004) was performed to help constrain the mobilized volume to be used in the runout analysis. The 2-D finite-difference program FLAC (Itasca 2005) was used for this purpose. The advantage of this approach is that predefinition of the rupture surface is not required, allowing its location and shape to be modeled as a function of the shear stress distribution in the slope and resulting elasto-plastic yielding of elements (Eberhardt et al. 2004). Discontinuities are treated implicitly in terms of their effect on reducing the rock mass strength of the equivalent continuum. This was deemed acceptable given that: (1) no geological structures were identified that could serve as a controlling release feature (foliation dips into the slope); (2) mapping showed the discontinuities to be of limited persistence; and (3) the primary objective was to obtain an upper bound estimate of the maximum slide volume. The treatment of a rock mass as an equivalent continuum of course discounts the explicit role of discontinuities in controlling the specific path taken by the rupture surface. However, in cases where the discontinuities are nonpersistent and serve

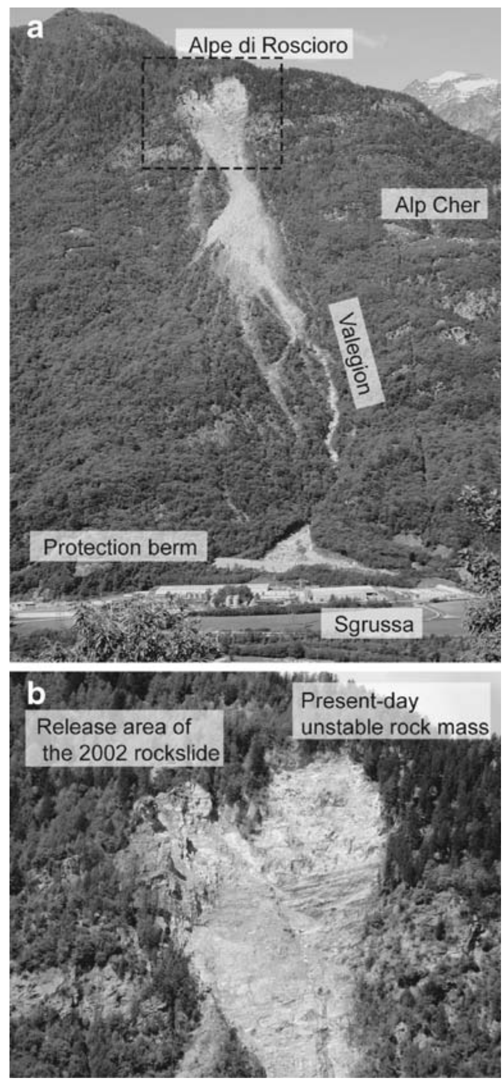


**Fig. 2** **a** Photo of the study site (situation after the 2002 rockslides, photo by G. Valenti). **b** Close-up of the scar region with the release area of the 2002 rockslide and the present-day unstable rock mass (photo by G. Valenti), outlined in (**a**). The left side of the scarp region was formed during the 2002 rockslide event, the right side is the front of the unstable rock mass

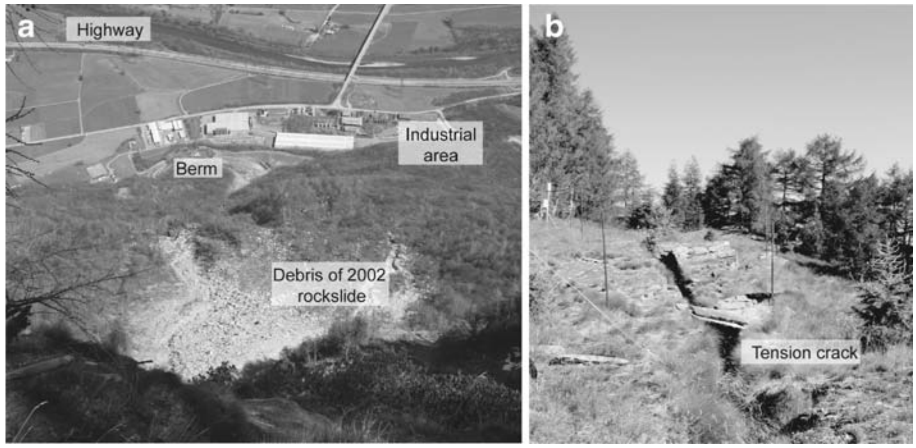


**Fig. 3** **a** View from the Alpe di Roscioro into the valley and the industrial area Sgrussa. **b** Tension crack on the Alpe di Roscioro

more to form step-paths of a deeper-seated rupture surface, continuum modeling has been shown to be sufficiently effective in providing an estimate of the depth of failure (Eberhardt 2008), especially when constrained by a tension crack at the top of the slope as in the case of Alpe di Roscioro.

### Model setup

The Alpe di Roscioro model was developed using data collected during the field investigation. The problem domain was defined based on the surface topography and key geological units (as depicted in Fig. 4), and the corresponding equivalent continuum rock mass properties were estimated based on typical values scaled to account for each unit's respective rock mass quality (after Hoek and Brown 1997). The model input parameters that were used are listed in Table 1. The amphibolites were characterized as being a good quality rock mass, the augengneisses as an average quality rock mass, the banded gneisses as an average-poor quality rock mass and the schists as a poor quality rock mass. Accordingly, a Mohr-Coulomb elasto-plastic yield criterion was used for the weaker, more deformable rock units, and a strain-softening yield criterion (i.e., decreasing strength as a function of increasing plastic strain) was used for the stronger units that were expected to behave in a more brittle manner. For this analysis, only the cohesion and tensile strengths were varied to simulate a brittle response; as shown by Eberhardt et al. (2004), the brittle failure process in crystalline rock is one that is dominated by cohesion loss.

Pore pressures were added to the model based on a water table indicated by the mapped springs at the contact between the banded gneisses and schists.

### Modeling results

The model results are presented in Fig. 7. These show the failure process initiating at the toe of the rock slope along the weak schist layer (Fig. 7a). Movement at the toe and the redistribution of shear stresses to elements surrounding those that have yielded then sets off a chain reaction, where accumulated shear strains above the schists lead to localization and the progressive development of a rupture surface. With increasing slope displacement, the failure surface then progresses from one driven by yield in shear (Fig. 7b) to increased extensional strain and failure in tension at the head of the slope (Fig. 7c). Here the location and mechanism (i.e., tension) of the modeled rupture surface agrees with that mapped on surface in the form of a large tension crack (Fig. 3a), providing a degree of model validation.

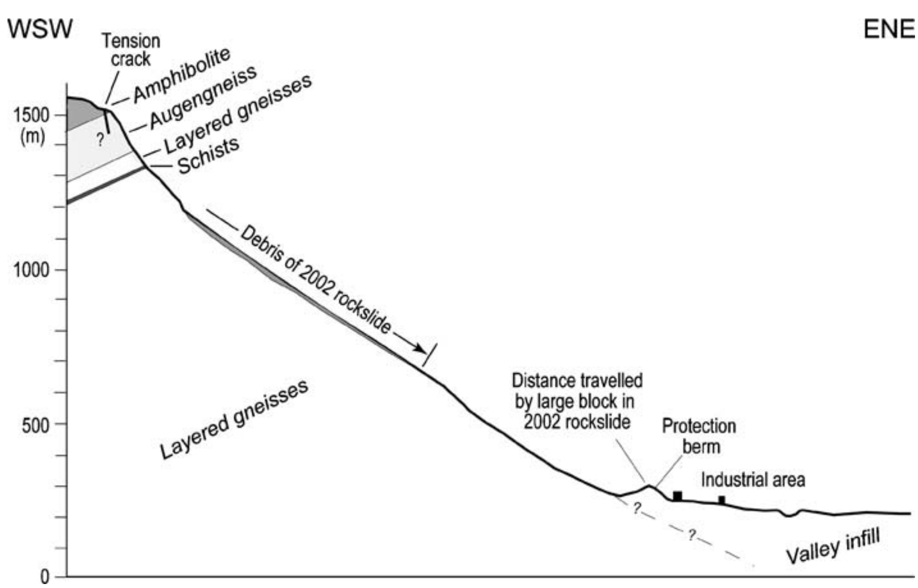


**Fig. 4** Geological cross-section through the investigated slope along the Valegion channel

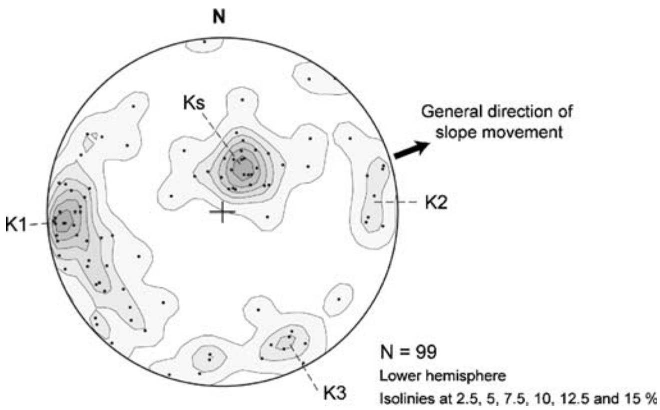


**Fig. 5** Fracture orientation distribution in a lower hemisphere projection. Fracture set Ks is oriented parallel to foliation and three steep fracture sets (K1-3) are present

Again, although these results disregard the importance of discontinuities in controlling the path of the rupture surface, they do provide a clear picture of strain localization and the development of a rupture surface delimiting the depth of failure. Comparable instability models have been used to explain other slope instabilities in massive rocks with underlying weaker layers (e.g., Gruner 2004). Yet to date, monitoring and mapping data are too limited to clearly identify the acting instability mechanisms. As such, the model provides a first estimate of the maximum depth of the unstable rock mass, and it was concluded that the unstable rock mass most likely extends down to the weak schist layers. Accordingly, a volume of unstable rock of 680,000 m$^3$ was calculated and used as a worst-case scenario for subsequent 2-D and 3-D runout analyses carried out for the hazard assessment.

## Runout simulation

### Method

The 2-D dynamic analysis code DAN (Hungr 1995), and its 3-D extension DAN3D (McDougall and Hungr 2004), were used to predict runout scenarios for the investigated rock slope hazard. The DAN model is based on a Lagrangian solution of the St. Venant shallow flow equations, incorporating earth pressure theory to simulate the motion of earth materials along a user-prescribed slope profile and a path width function. Several rheological models are available to treat basal flow resistance (Hungr 1995). Because the width of the landslide path is a required user input, the DAN code has generally been applied to back analyses to assess the mechanisms involved in destructive rock avalanches or debris flows (e.g., Evans et al. 2001; Hungr 2002; Smith et al. 2006; Evans et al. 2007). However, DAN has also been applied to forward runout prediction modeling in certain cases (Hungr and Evans 1996; Pirulli 2004).

DAN3D retains the key features of DAN but implements a numerical method adapted from smoothed particle hydrodynamics to allow it to simulate landslide runout across complex 3-D terrain (McDougall and Hungr 2004; McDougall 2006). Thus, with proper calibration for input parameters corresponding to a given landslide type, the model has the ability to provide first-order predictions of landslide flow behavior, including direction, velocity, depth, and runout extent. The two programs produce comparable results when applied to the same runout case histories with the same input parameters (Hungr and McDougall 2008). The calibration procedure benefits from the simplicity of the assumed rheological models. Generally, only one or two adjustable parameters need to be determined. For "dry" rock slides of limited volume, where entrainment of saturated substrate does not play a role, the frictional model with a basal bulk friction angle of over 30° has been successful (Hungr et al. 2005).

The runout analysis was first carried out using DAN to take advantage of the computational efficiency of the 2-D code. Two different volume scenarios were investigated based on the modeling results and field observations (Fig. 8). The larger volume of 680,000 m$^3$ represents a complete failure of the unstable rock slope. This value is based on a conservative assumption of failure occurring coherently as a single volume and was required given the sensitive presence of the factory below the unstable rock slope. It corresponds to the slide volume determined through the FLAC slope stability analysis (previously described). The smaller volume of 260,000 m$^3$ represents scenarios in which only a portion of the rock mass between the Alpe di Roscioro and schist band at depth (Fig. 4) fails. This model was chosen with respect to the failure mechanism of the 2002 rockslide, which occurred in a piecemeal fashion.

**Fig. 6** Surface fracture opening at the tension crack on the Alpe di Roscioro. The automatically recorded extensometers (1–4) are positioned along the tension crack from south (E1) to north (E4). The monitoring data was provided by G. Valenti and M. Franzi

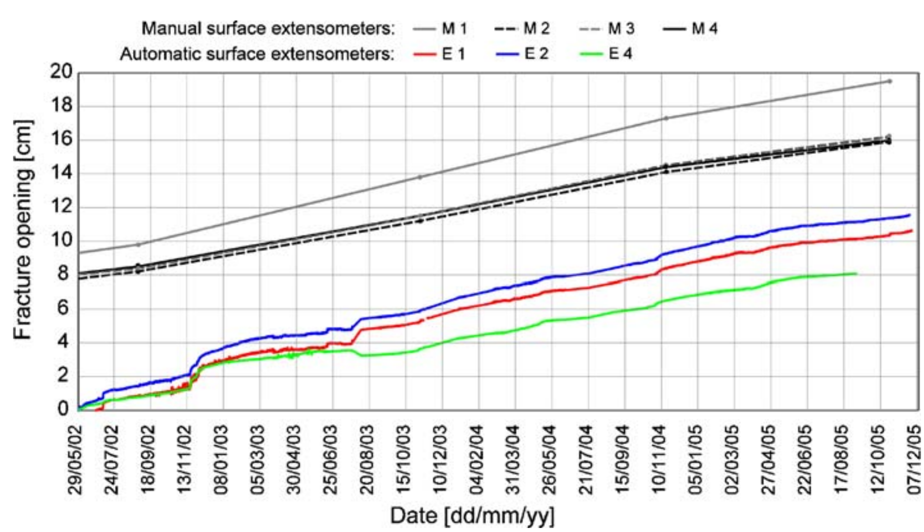

**Table 1** Parameters used for FLAC modelling with a strain-softening constitutive model

| | | Amphibolites | Augengneisses | Layered gneisses | Schists |
|---|---|---|---|---|---|
| Young's Modulus, $E$ | (GPa) | 20 | 20 | 20 | 15 |
| Poisson's ratio, $\nu$ | (–) | 0.25 | 0.25 | 0.25 | 0.3 |
| Density, $\rho$ | (kg/m$^3$ ) | 2,600 | 2,600 | 2,600 | 2,600 |
| Friction, $\phi$ | (°) | 40 | 35 | 25 | 20 |
| Cohesion, $c$ | (MPa) | 10, 5, 1, 0.5[a] | 1, 0.5, 0.1, 0.05[a] | 0.5 | 0.1 |
| Tensile strength, $T_o$ | (MPa) | 1.5, 0.5, 0.25, 0[a] | 0.75, 0.25, 0.05, 0 * | 0.1 | 0.05 |

[a] Strain softening values corresponding to plastic strains of 0, 0.0005, 0.001, and 0.002, respectively

All runout prediction models assumed a frictional rheological model (Hungr 1995). The internal frictional angle was chosen as 35°, as appropriate for shearing of dry angular rock fragments, and not varied between runs. The basal friction angle for the forward prediction was derived from back-analyses of rockslides with approximately the same volume, material and topographic setting (see "Model calibration" section).

These 2-D results were followed up with a series of DAN3D models to test the validity of the 2-D assumption of travel path and width. The DAN3D formulation does not require any predefinition of the failure path, only the 3-D surface topography. For this analysis, an existing 1:25,000 digital elevation model of the slope was used. Similar to the 2-D simulation, a frictional rheology was chosen.

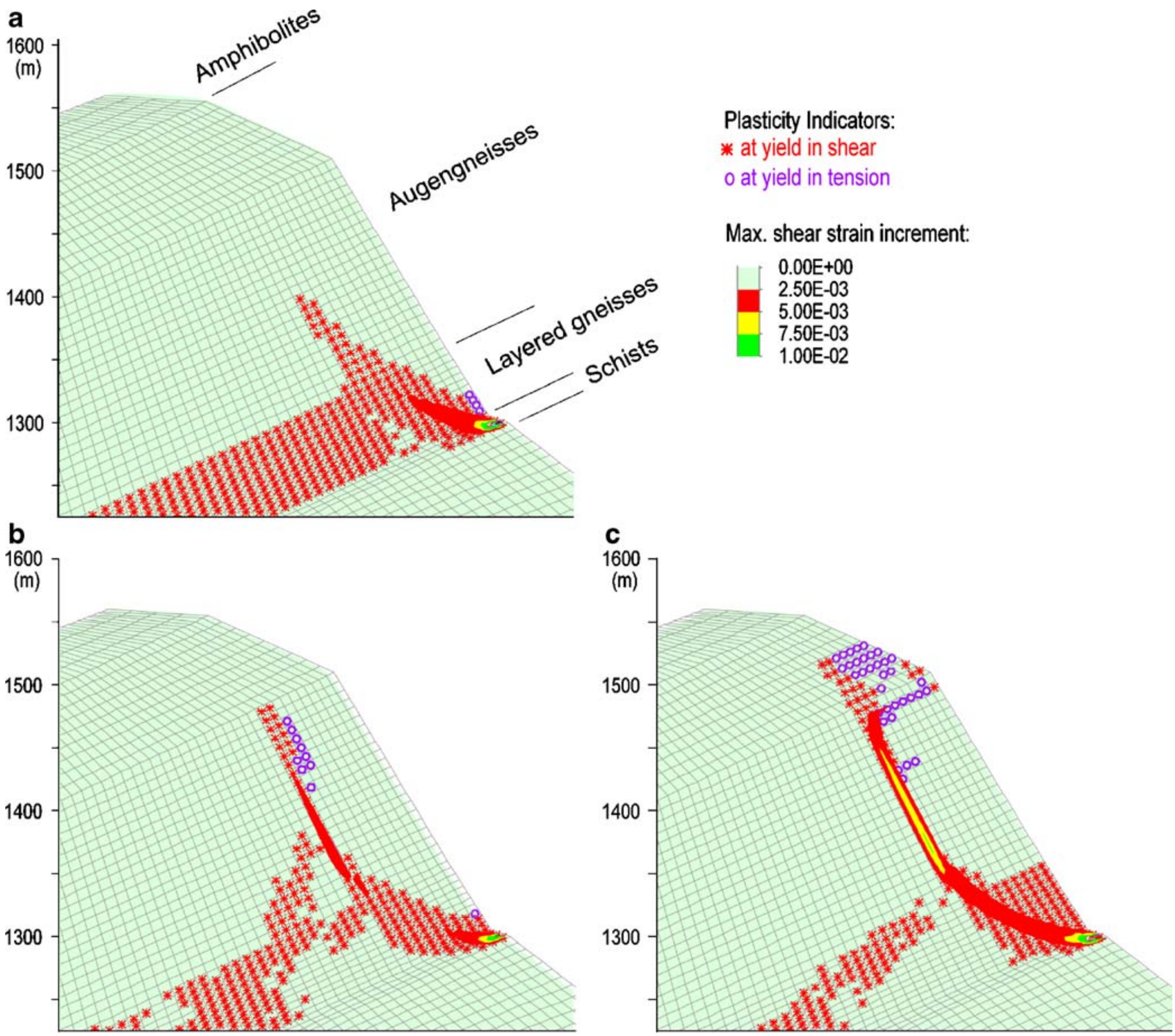


**Fig. 7** Numerical modeling results using the continuum-based finite-difference code FLAC

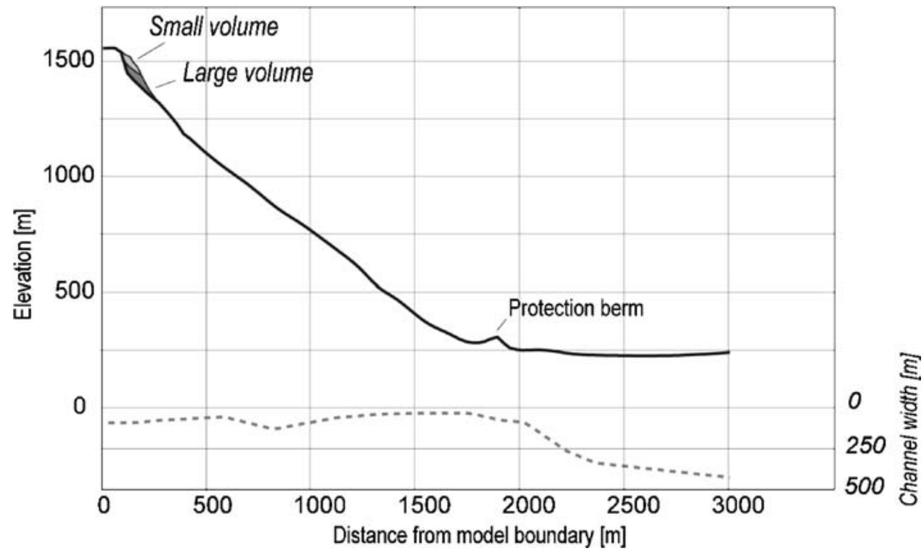


**Fig. 8** DAN model for the runout simulation involving two possible rockslide volumes

### Model calibration

The key focus of model calibration was the value of the basal friction angle. As Table 2 shows, only a few values of back-calculated basal friction angle are provided in the literature for rockslides with comparable volumes, material, and slope characteristics. A series of four additional back analyses, based on documented rockslides in Switzerland, were completed to supplement these values (see Fig. 1 for locations and Fig. 9 for cross-sections). All four have been documented as involving rapid slope failures and were somewhat larger than the present case. The Airolo and Zarera slides resulted in the destruction of parts of the villages below the release area (Eisbacher and Clague 1984), and the impacts of the two 1996 Sandalp events were detectable in seismic records (Keusen 1998). The results from these back analyses (Fig. 9) provided values for basal friction angle ranging between 25° and 35° (Table 3). The effects of pore pressure are accounted for implicitly in the calibrated basal friction angle (see Hungr 1995). Entrainment along the path was considered negligible for each of these cases.

It should be noted that the 2002 rockslide from the Alpe di Roscioro, which lasted several hours, was not used for the back analysis as failure did not occur coherently as a single volume but took place over a longer duration as a series of smaller rock fall events.

### Results and discussion

The forward prediction of 2-D runout distances for the two failure volumes and different base friction angles are shown in Fig. 10. The 2-D path was assumed to follow the main morphological feature at the bottom of the slope—the Valegion channel, and included the presence and influence of the protection berm (Fig. 8). For the upper limit basal friction angle value (35°), the rockslide debris stops at the protection berm. However, basal friction angles below this value all resulted in the slide debris overrunning the berm and impacting the industrial area. For the larger rockslide volume, the runout even reaches and buries the main highway close to Preonzo.

The results of the DAN3D models are shown in Fig. 11. The rock debris was seen to split into two streams before it reaches the Valegion channel. For models adopting the upper limit friction angle of 35°, the deposit covers a larger area higher up on the slope, but only a reduced volume enters the lower channel. For the lower friction angles, a larger volume becomes channelized by the Valegion channel, resulting in an even longer runout distance. Thus, for lower friction angles, the choice of a travel path along the Valegion channel seems reasonable.

Next to the behavior of the rockslide debris, as a function of the basal friction angle, the 3-D results show that the degree of spreading of the path and the volume of the channelized slide debris (i.e., the 3-D topographical controls) have a significant impact on the runout predictions. Consequently, an additional series of 2-D models examined the influence of the runout path geometry at the base of the slope in detail for the case of the larger volume rockslide event and for a 30° basal friction angle. In order to account for the possibility that the large-volume event may entrain saturated material from the valley bottom deposits, a reduced bulk friction angle of 20° was used on the horizontal segment of the path. This is intended to simulate partial liquefaction (undrained conditions) of the alluvial soil on the

**Table 2** DAN base friction angles from literature

| Rockslide | Analysis by | Volume ($m^3$) | Rock type | Slope (°) | Friction angle (°) |
|---|---|---|---|---|---|
| Turbid Creek | Pirulli 2004 | 940,000 | Pyroclastic | –/– | 17.5 |
| Flims | Hungr and Evans 1996 | 100,000 | Limestone | –/– | 23 |
| Eagle Pass[a] | Hungr and Evans 2004 | 75,000 | Gneiss | 26 | 30 |
| Ceppo Morelli[b] | Pirulli 2004 | 1,000,000 | Gneiss | 30 | 30 |

[a] Change of rheological model in lower part of the slope[b] Prediction–/– not specified

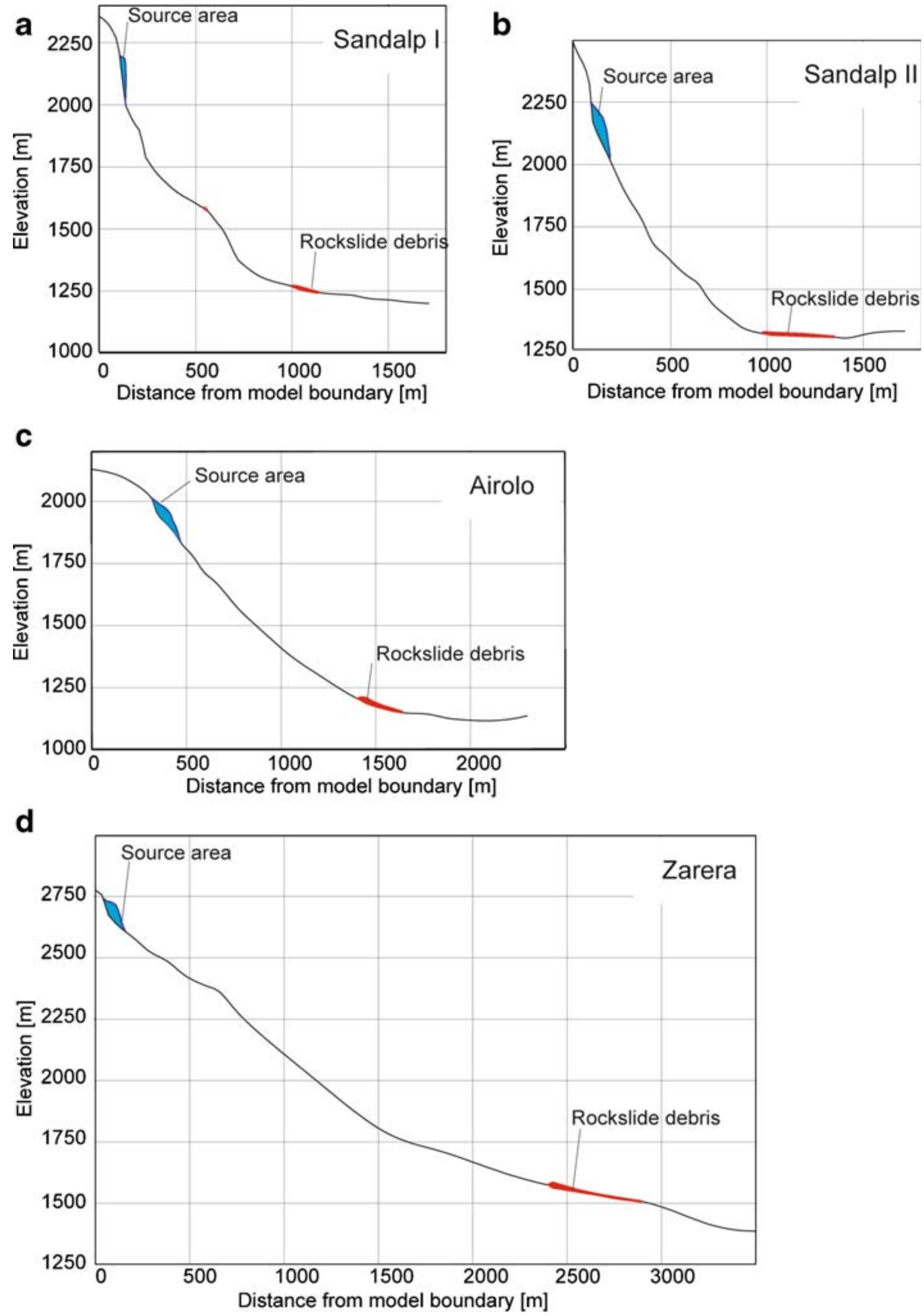


**Fig. 9** Case histories from Switzerland for calibration of DAN base friction angles

valley floor and is based on the authors' previous experience back-analyzing rock avalanches that impact wet alluvium. The results for these model runs, summarized in Fig. 12, show that even though the rockslide runout distance decreases with increasing spreading of the debris, the industrial area is still impacted in each case.

## Conclusions

Two- and three-dimensional dynamic runout analyses show that for a large volume rockslide event (>300,000 m$^3$), involving an unstable rock slope above an industrial site near Preonzo, Switzerland, and even for a smaller volume under specific

**Table 3** DAN base friction angles from back analysis of rockslides in Switzerland

| Rockslide | Documentation by | Volume (m$^3$ ) | Rock type | Slope (°) | Friction angle (°) |
|---|---|---|---|---|---|
| Zarera (13.06. 1486) | Eisbacher and Clague 1984 | 500–800,000 | Amphibolitic gneisses | 30 | 25 |
| Airolo Sasso Rosso (27.12.1898) | Eisbacher and Clague 1984 | 500,000 | Gneisses and schists | 30–25 | 32 |
| Sandalp (24.01.1996) | Keusen 1998 | 470,000 | Limestone | 30–40 | 33–35[a] |
| Sandalp (03.03.1996) | Keusen 1998 | 1,750,000 | Limestone | 60–40 | 30* |

[a] Runout depending mostly on pore pressure and entrainment in the valley section of the travel path

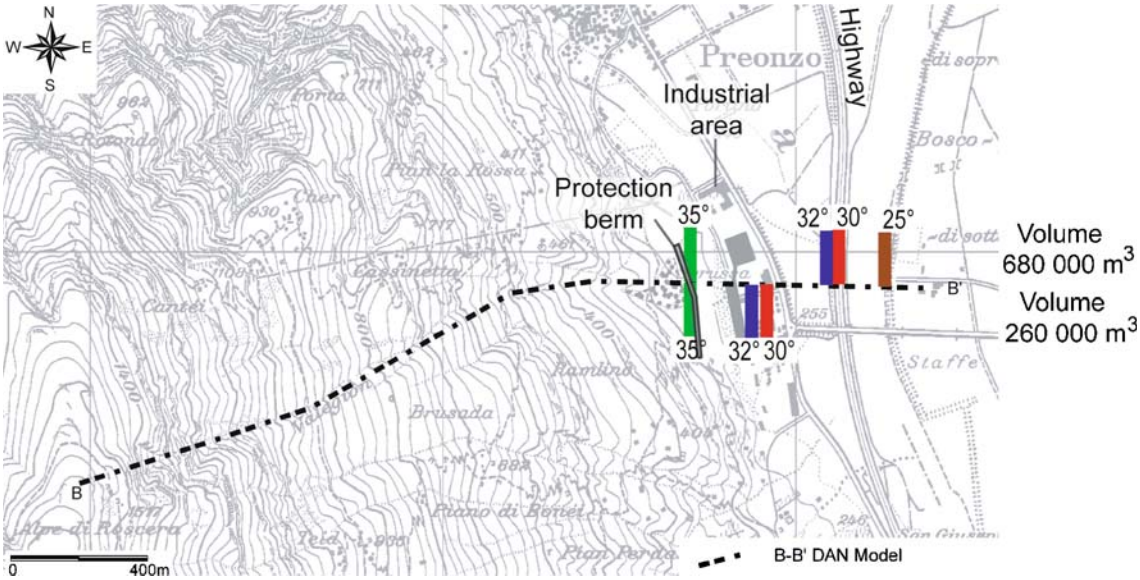


**Fig. 10** Maximum runout distances for the two different rock volumes in dependence of the friction angle of the underground. The analyzed travel path is indicated by the *dotted line*. Contour map is reproduced by permission of Swisstopo (BA091024)

**Fig. 11** Maximum flow depths simulated with DAN3D (shown at 5 m contour intervals). **a** Frictional rheology, 30° friction angle. **b** Frictional rheology, 35° friction angle

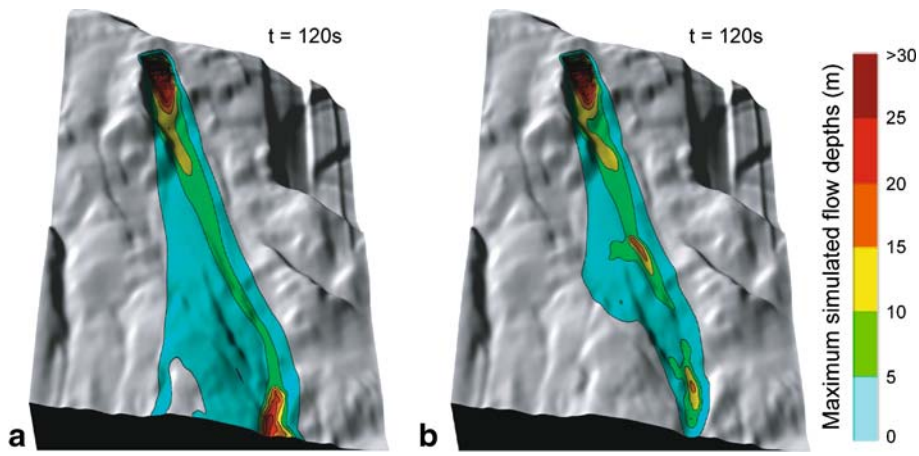


**Fig. 12** Maximum extent of the rockslide runout for the large rock volume in dependence of the channel width in the valley for constant friction angle of 30° on the slope and 20° in the valley. Contour map underlay is reproduced by permission of Swisstopo (BA091024)

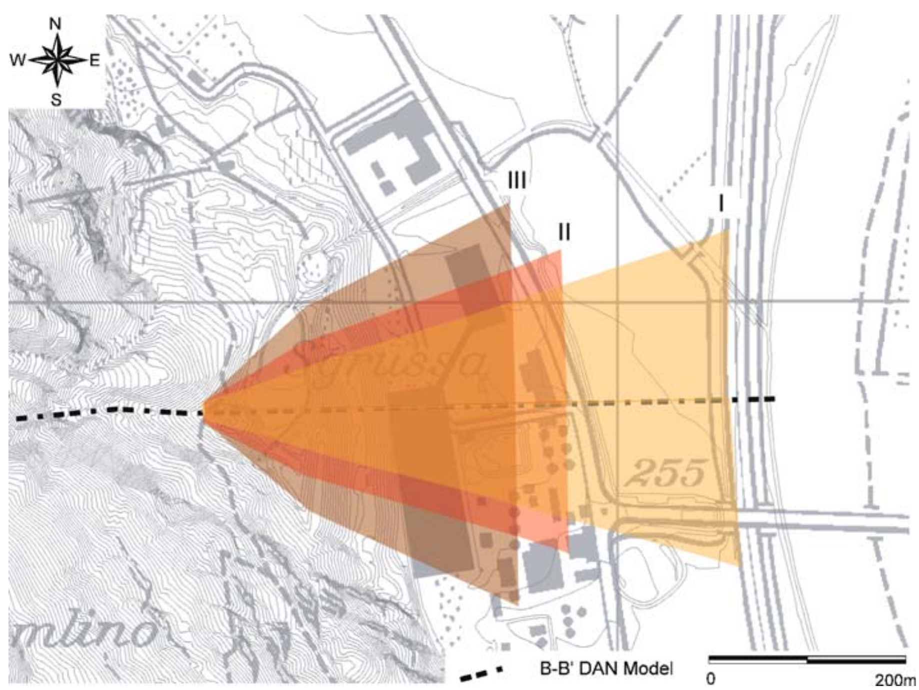

conditions, the industrial area below the unstable slope is not sufficiently protected by a berm and catchment dam built in 2002. This conclusion, however, is dependent on several assumptions and model simplifications involving the volume of the slope failure, the travel path geometry, and the rheological model and parameters used to simulate the rockslide runout. Geological mapping and numerical modeling were used to gain an understanding of the acting instability mechanism and to constrain the failure volume, whereas a number of calibration simulations were used to constrain the input parameters required by the rheological model used for the runout analysis.

The investigation and analysis procedure followed here was largely shaped by the practical challenges faced when dealing with geological uncertainty and limited data for which an answer still must be provided. The runout prediction had to be based on simplifying assumptions, cross-validation with other models, and several parametric studies. Most of the assessed scenarios indicate a significant risk for the industrial area in the event of a rockslide

Thus, the results also emphasize the importance of an operating early warning system implemented for the unstable Alpe di Roscioro slope. Together, these will help provide a basis for the local authorities to define hazard zones, design necessary countermeasures (e.g., early warning trigger thresholds, evacuation plans, etc.) and to aid further development plans for the community of Preonzo.

### Acknowledgements

The authors want to thank Giorgio Valenti and Marco Franzi (Sezione Forestale Cantonale, Ticino, Bellinzona) for their support, valued discussions, and for providing access to all previous mapping and monitoring data. This study was financed by the local and national authorities.

### References

Eberhardt E (2008) Twenty-Ninth Canadian Geotechnical Colloquium: The role of advanced numerical methods and geotechnical field measurements in understanding complex deep-seated rock slope failure mechanisms. Can Geotech J 45(4):484–510 doi:10.1139/T07-116

Eberhardt E, Stead D, Coggan JS (2004) Numerical analysis of initiation and progressive failure in natural rock slopes - the 1991 Randa rockslide. Int J Rock Mech Min Sci 41 (1):68–87 doi:10.1016/s1365-1609(03)00076-5

Eisbacher GH, Clague JJ (1984) Destructive mass movements in high mountains: Hazard and management. Paper 84-16. Minister of Supply and Services, Ottawa, 230 pp

Evans SG, Hungr O, Clague JJ (2001) Dynamics of the 1984 rock avalanche and associated distal debris flow on Mount Cayley, British Columbia, Canada; implications for landslide hazard assessment on dissected volcanoes. Eng Geol 61(1):29–51

Evans SG, Guthrie RH, Roberts NJ, Bishop NF (2007) The disastrous February17, 2006 rock avalanche on Leyte Island, Philippines: a catastrophic landslide in tropical mountain terrain. Nat Hazards Earth Syst Sci 7:89–101

Geertsema M, Clague JJ, Schwab JW, Evans SG (2006) An overview of recent large catastrophic landslides in northern British Columbia, Canada. Eng Geol 83(1-3):120–143 doi:10.1016/j.enggeo.2005.06.028

Gruner U (2004) Klima und Sturzereignisse in Vergangenheit und Zukunft. Bull Angew Geologie 9(2):23–37

Hoek E, Brown ET (1997) Practical estimates of rock mass strength. Int J Rock Mech Min Sci 8:1165–1186 doi:10.1016/S0148-9062(97)00305-7

Hungr O (1995) A model for the runout analysis of rapid flow slides, debris flows, and avalanches. Can Geotech J 32:610–623 doi:10.1139/t95-063

Hungr O (2002) Rock avalanche occurrence, process and modelling. In: Evans SG, Scarascia Mugnozza G, Storm A, Hermanns RL (eds) Landslides from massive rock slope failure, NATO Science Series. Springer, Dordrecht, pp 243–266

Hungr O, Evans SG (1996) Rock avalanche runout prediction using a dynamic model. In: Senneset K (ed) International Symposium on Landslides, Trondheim, pp 233–238

Hungr O, Evans SG (2004) Entrainment of debris in rock avalanches: an analysis of a long run-out mechanism. Geol Soc Am Bull 116(9–10):1240–1252

Hungr O, McDougall S (2009) Two numerical models for landslide dynamic analysis. Comput Geosci (in press).

Hungr O, Corominas J, Eberhardt E (2005) Estimating landslide motion mechanism, travel distance and velocity. In: Hungr O, Fell R, Couture R, Eberhardt E (eds) Landslide Risk Management. Taylor & Francis, London, pp 99–128

Itasca (2005) FLAC - Fast Langrangian Analysis of Continua. Itasca Consulting Group, Minneapolis

Keusen HR (1998) Die Bergstürze auf der Sandalp 1996—Risikobeurteilung und Gefahrenmanagement. Bull Angew Geologie 3(1):89–102

McDougall S (2006) A new continuum dynamic model for the analysis of extremely rapid landslide motion across complex 3D terrain. PhD thesis Thesis. University of British Columbia, Vancouver, 253 pp

McDougall S, Hungr O (2004) A model for the analysis of rapid landlside motion across three-dimensional terrain. Can Geotech J 41(6):1084–1097 doi:10.1139/t04-052

Nadim F, Kjekstad O, Peduzzi P, Herold C, Jaedicke C (2006) Global landslide and avalanche hotspots. Landslides 3(2):159–173 doi:10.1007/s10346-006-0036-1

Petley DN, Dunning SA, Rosser NJ (2005) The analysis of global landslide risk through the creation of a database of worldwide landslide fatalities. In: Hungr O, Fell R, Couture R, Eberhardt E (eds) Landslide risk management. Taylor & Francis, London, pp 367–373

Pirulli M (2004) Numerical analysis of three potential rock avalanches in the Alps. Felsbau 22:32–38

Schindler C, Cuénod Y, Eisenlohr T, Joris CL (1993) Die Ereignisse vom 18. April und 9. Mai 1991 bei Randa (VS)—ein atypischer Bergsturz in Raten. Eclogae Geol Helv 86 (3):643–665

Smith GM, Davies TR, McSaveney MJ, Bell DH (2006) The Acheron rock avalanche, Canterbury, New Zealand—morphology and dynamics. Landslides 3:62–72 doi:10.1007/s10346-005-0012-1

Stead D, Eberhardt E, Coggan JS (2006) Developments in the characterization of complex rock slope deformation and failure using numerical modelling techniques. Eng Geol 83:217–235 doi:10.1016/j.enggeo.2005.06.033

**H. Willenberg · S. Loew**
Geological Institute, Swiss Federal Institute of Technology, ETH Hoenggerberg,
CH-8093 Zürich, Switzerland

**E. Eberhardt (✉) · O. Hungr**
Geological Engineering, Department of Earth and Ocean Sciences,
University of British Columbia,
Vancouver, BC V6T 1Z4, Canada
e-mail: erik@eos.ubc.ca

**S. McDougall**
BGC Engineering Inc.,
500-1045 Howe St.,
Vancouver, SP V6Z 2A9, Canada

*Present address:*
**H. Willenberg**
Matousek, Baumann & Niggli AG,
Maederstr. 8,
5401 Baden, Switzerland